Available online at www.sciencedirect.com
SCIENCE DIRECT®
Journal of Molecular Structure 660 (2003) 1–13
Journal of MOLECULAR STRUCTURE
www.elsevier.com/locate/molstruc

Synthesis, characterization and interaction mechanism of new oxadiazolo-phthalimides as peripheral analgesics. IV☆

Roberto Antunes[a,1,2], Hildson Batista[a], Rajendra M. Srivastava[a,*], George Thomas[b], Clidenor C. Araújo[b], Ricardo L. Longo[a], Hélio Magalhães[c], Marcelo B.C. Leão[a2], Antônio C. Pavão[a]

[a]*Departamento de Química Fundamental, CCEN, Universidade Federal de Pernambuco, 50740-540 Recife, PE, Brazil*
[b]*Laboratório de Tecnologia Farmacêutica, Universidade Federal da Paraíba, João Pessoa, PB, Brazil*
[c]*Departamento de Engenharia de Sistemas, Universidade Federal de Pernambuco, 50740-540 Recife, PE, Brazil*

Received 5 December 2002; revised 2 June 2003; accepted 10 June 2003

Abstract

The synthesis, characterization and spectroscopic studies of compounds **6a–g** with analgesic activity is described. A new model of interaction between the drug and the enzyme is suggested. Application of the Resonance Valence Bond theory led us to propose, for the first time, an entirely new mechanism involving an electron transfer from the amino acid residue of the enzyme to the drug. Theoretical studies of various transition states involved in the interaction mechanism employing the semi-empirical molecular orbital calculations (AM1 method) have been carried out. This article also deals with an extensive study of the structure–activity relationships of seven oxadiazolo-phthalimides **6a–g**.

Keywords: Phthalimide derivatives; 1,2,4-Oxadiazoles; Analgesic; Antiinflammatory

1. Introduction

Signaling molecules produced in the vicinity of the damaged tissues usually cause the inflammation process. To control pain due to inflammation, analgesic drugs are administered, which can be classified as narcotic, when acting on the central nervous system, and non-narcotic or peripheral, when acting directly on the damaged tissue [1]. Peripheral analgesics are drugs that, independent of their mode of action, show a therapeutic effect by supressing the production of prostaglandins, which are lipids responsible for inflammation and pain. Non-steroidal anti-inflammatory drugs (NSAIDs) [2] are examples of peripheral analgesics, since they block both isoforms COX-1 and COX-2 of the enzyme cyclooxygenase (COX). Acetylsalicylic acid (aspirin), for instance, binds irreversibly to the COX enzyme via an acetylation reaction [3,4], such that the production

☆ For analgesic activity of phthalimide derivatives, see part II, Ref. [14].

* Corresponding author. Tel.: +55-81-3271-8443; fax: +55-81-3271-8442.
E-mail address: rms@ufpe.br (R.M. Srivastava).

[1] Taken in part from the Ph.D. thesis of R. Antunes, 1998, Universidade Federal de Pernambuco, Recife.

[2] Present Address: Departamento de Química, Universidade Federal Rural de Pernambuco, Recife.

0022-2860/$ - see front matter © 2003 Elsevier B.V. All rights reserved.
doi:10.1016/S0022-2860(03)00418-6

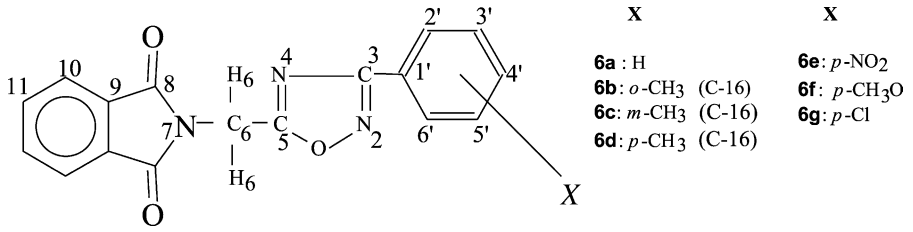

Fig. 1. Seven new oxadiazolo-phthalimides with analgesic and antiinflammatory properties.

of pain-inducing mediators that act on nerve cells is halted. Other NSAIDs such as indomethacin or ibuprophen produce a reversible inhibition [5], competing with arachidonic acid for the active site of the enzyme.

This pain-inducing mechanism has been actively studied and, recently, it has been shown [6] that it is not a nerve signal but a signal transported in the bloodstream that triggers the central nervous system to produce molecules such as interleukin-1β and release them into the cerebrospinal fluid. Interleukin-1β causes nerve cells to start producing COX, thereby initiating pain signal within the nervous system. When NSAIDs are injected directly into the cerebrospinal fluid, they inhibit COX there and make the inflammation less painful. Accordingly, this class of painkillers had heretofore been thought to work exclusively outside the brain and should now be specifically designed to penetrate into the brain.

Although many of the NSAIDs possess analgesic and antiinflammatory properties, some of them have been used for the treatment of Alzheimer's disease [7] and also as anti-cancer agents [8,9]. Given the importance of these drugs, we have been dedicated in synthesizing new oxadiazole derivatives with analgesic and antiinflammatory activities, for instance, 3-[3-(phenyl)-1,2,4-oxadiazol-5-yl]propionic acid (POPA) has shown to possess both properties [10]. We have also been interested in phthalimide derivatives, since some studies revealed that thalidomide was efficient in the treatment of erythema nodosum leprosum (ENL), a sharp manifestation of the Hansen's disease [11,12]. In 1996, thalidomide has been reported to be efficient in another inflammatory process [13]. As a result, we have synthesized and evaluated the analgesic properties of several new oxadiazolo-phthalimides (Fig. 1, **6a**–**g**), and interestingly, all of them have shown significant analgesic and antiinflammatory properties [14]. This is a strong indication that these substances act like NSAIDs, and therefore are able to inhibit the PGHS or COX enzyme. On the other hand, the present compounds do not have a carboxylate group, which is present in most of the classic NSAIDs. Thus, we propose that these new substances can inhibit COX-2, and the present work describes a qualitative chemical model for the interaction between COX-2 and oxadiazolo-phthalimides, based upon molecular orbital calculations.

2. Experimental procedure

2.1. General experimental methods

Melting points were obtained with a Digital Electrothermal IA 9100 equipment and are uncorrected. ^{1}H (300 MHz) and ^{13}C (75.43 MHz) NMR spectra were recorded with a Varian Unity Plus 300 MHz spectrophotometer using an appropriate solvent and tetramethylsilane (TMS) as an internal reference. The numbering system used for ^{1}H and ^{13}C spectral assignments of compounds **6a**–**g** is given in Fig. 1. Infrared spectra were recorded with a Brucker IFS 66 instrument. Sanyo domestic microwave oven (model EM-3500B, 1350W/2450 MHz) was used for the synthesis of compound **3**. Silica gel G plates (Merck) with fluorescent indicator PF_{254} were employed for thin-layer chromatography, using chloroform/ethyl acetate (85%/15%) and the plates was revealed under ultraviolet light.

2.2. Chemistry

2.2.1. N-[3-(Phenyl)-1,2,4-oxadiazol-5-yl-methyl] phthalimide (**6a**)

To compound **3** (9.3 mmol) dissolved in DME (8.0 ml) was added DCC (7.4 mmol) and an appropriate arylamidoxime **4a** (9.3 mmol) in DME (8.0 mL) and the reaction mixture was stirred for 30 min at room temperature and then refluxed for 16 h [15]. The solvent was removed under vacuum and the residue chromatographed on a silica gel column using chloroform/*n*-hexane (70%/30%, v/v) as eluent, which provided **6a** as a colorless solid. Chromatographically pure material was crystallized and recrystallized from chloroform until the melting point became constant: mp 189–190 °C, yield 51%; IR (KBr) 1776, 1723, 1598, 1572, 1107 and 949 cm^{-1}; ^1H NMR ($CDCl_3$) δ 8.01–8.03 (m, 2H, H-2′ and H-6′), 7.95 (AA′BB′ system, 2H, $J_{10,11} = 5.6$ Hz, $J_{10,12} = 3.2$ Hz, H-10, H-13); 7.79 (AA′BB′ system, 2H, $J_{11,12} = 5.6$ Hz, $J_{11,13} = 3.2$ Hz, H-11, H-12) 7.41–7.48 (m, 3H, H-3′, H-4′ and H-5′), 5.18 (s, 2H, H-6 and H-6_t; ^{13}C NMR ($CDCl_3$) δ 173.67 (C-5), 168.59 (C-3), 166.93 (C-15), 134.51 (C-10), 131.79 (C-9), 131.31 (C-4′), 128.75 (C-3′,C-5′) 127.52 (C-2′, C-6′) 126.19 (C-1′),123.89 (C-11) 33.59 (C-6). Anal. calcd for $C_{17}H_{11}N_3O_3$ (305.08): C, 66.87; H, 3.63; N, 13.77. Found: C, 66.67; H, 3.70; N, 13.74. Other 1,2,4-oxadiazoles were prepared, purified and characterized similarly.

2.2.2. N-[3-(o-Tolyl)-1,2,4-oxadiazol-5-yl-methyl] phthalimide (**6b**)

Crystallized from chloroform, yield 49%; mp 132 °C; IR (KBr): 1772, 1718, 1602, 1569, 1107 and 947 cm^{-1}; ^1H NMR ($CDCl_3$) δ 7.88–7.91 (m, 1H, H-6′), 7.94 (AA′BB′ system, 2H, $J_{10,11} = 5.4$ Hz, $J_{11,13} = 3.3$ Hz, H-10, H-13); 7.79 (AA′BB′ system, 2H, $J_{11,12} = 5.4$ Hz, $J_{11,13} = 3.0$ Hz, H-11, H-12); 7.21–7.38 (m, 3H, H-3′, H-4′ and H-5′), 5.18 (s, 2H, H-6 and H-6_t), 2.57 (s, 3H, CH_3-Ar); ^{13}C NMR ($CDCl_3$) δ 172.66 (C-5), 169.13 (C-3), 166.94 (C-15), 138.26 (C-1′), 134, 49 (C-11), 131.86 (C-9), 131.28 (C-3′), 130.68 (C-5), 130.17 (C-6′) 125.87 (C-4), 125.52 (C-2′), 123.86 (C-11), 33.62 (C-6), 22.01 (CH_3-Ar). Anal. calcd for $C_{18}H_{13}N_3O_3$ (319.30): C, 67.69; H, 4.11; N, 13.17. Found: C, 67.40; H, 4.04; N, 12.98.

2.2.3. N-[3-(m-Tolyl)-1,2,4-oxadiazol-5-yl-methyl] phthalimide (**6c**)

Crystallized from chloroform, yield 56%; mp 144–145 °C; IR (KBr): 1773, 1723, 1578, 1521, 1109 and 948 cm^{-1}; ^1H NMR ($CDCl_3$) δ 7.81–7.84 (m, 2H, H-2′ and H-6′), 7.94 (AA′BB′ system, 2H, $J_{10,11} = 5.2$ Hz, $J_{10,12} = 3.2$ Hz, H-10, H-13); 7.79 (AA′BB′ system, 2H, $J_{11,12} = 5.2$ Hz, $J_{11,13} = 3.2$ Hz, H-11, H-12); 7.28–7.35 (m, 2H, H-4′ and H-5′), 5.17 (s, 2H, H-6 and H-6_t), 2.38 (s, 3H, CH_3-Ar); ^{13}C NMR ($CDCl_3$) δ 173.54 (C-5), 168.65 (C-3), 166.88 (C-15), 138.52 (C-5′), 134.46 (C-10), 132.07 (C-4′), 131.75 (C-9), 128.63 (C-3′), 127.99 (C-6′), 126.00 (C-1′), 124.61 (C-2′), 123.84 (C-11), 33.54 (C-6), 21.23 (CH_3-Ar). Anal. calcd for $C_{18}H_{13}N_3O_3$ (319.30): C, 67.69; H, 4.11; N, 13.17. Found: C, 67.40; H, 4.03; N, 13.37.

2.2.4. N-[3-(p-Tolyl)-1,2,4-oxadiazol-5-yl-methyl] phthalimide (**6d**)

Crystallized from chloroform, yield 55%; mp 168.0–169 °C; IR (KBr): 1772, 1724, 1594, 1570, 1112 and 944 cm^{-1}; ^1H NMR ($CDCl_3$) δ 7.88–790 (m, 2H, H-2′ and H-6′), 7.92 (AA′BB′ system, 2H, $J_{10,11} = 5.4$ Hz, $J_{10,12} = 3.0$ Hz, H-10, H-13); 7.79 (AA′BB′ system, 2H, $J_{11,12} = 5.7$ Hz, $J_{10,12} = 3.0$ Hz, H-11, H-12); 7.21–7.24 (m, 2H, H-3′ and H-5′), 5.16 (s, 2H, H-6 and H-6_t), 2.38 (s, 3H, CH_3-Ar); ^{13}C NMR ($CDCl_3$) δ 173.46 (C-5), 168.62 (C-3), 166.90 (C-15), 141.64 (C-4′), 134.47 (C-10), 131.85 (C-9), 129.45 (C-3′, C-5′), 127.46 (C-2′, C-6′), 123.86 (C-11), 123.45 (C-1′), 33.60 (C-6), 21.52 (C-16). Anal. calcd for $C_{18}H_{13}N_3O_3 \cdot 1/2\ H_2O$ (328.29): C, 65.85; H, 4.30; N, 12.79. Found: C, 65.53; H, 4.01; N, 12.57.

2.2.5. N-[3-(p-Nitrophenyl)-1,2,4-oxadiazol-5yl-methyl]phthalimide (**6e**)

Crystallized from acetone, yield 20%; mp 218–219 °C; IR (KBr): 1777, 1721, 1608, 1572, 1108 and 943 cm^{-1}; ^1H NMR ($CDCl_3$) δ 8.28 (AA′BB′ system, 4H, H-2′, H-3′, H-5′ and H-6′), 7.98 (AA′BB′ system, 2H, $J_{10,11} = 5.7$ Hz, $J_{10,12} = 3.0 \times$ Hz, H-10, H-13); 7.84 (AA′BB′ system, 2H, $J_{11,12} =$ 3.2 Hz, H-11, H-12); 5.22 (s, 2H, H-6 and H-6_t);

^{13}C NMR ($CDCl_3$) δ 174.65 (C-5), 167.09 (C-3), 166.88 (C-15), 149.51 (C-4′), 134.66 (C-10), 131.74 (C-1′), 131.08 (C-9), 128.57 (C-2′, C-6′), 124.03 (C-11), 124.00 (C-3′, C-5′), 33.55 (C-6). Anal. calcd for $C_{17}H_{10}N_4O_5$ (350.16): C, 58.29; H, 2.88; N, 15.99. Found: C, 58.25; H, 2.91; N, 15.81.

2.2.6. N-[3-(p-Anisyl)-1,2,4-oxadiazol-5-yl-methyl] phthalimide (**6f**)

Crystallized from methanol, yield 82%; mp 157–158 °C; IR (KBr): 1774, 1729, 1614, 1593, 1113 and 946 cm^{-1}; ^{1}H NMR ($CDCl_3$) δ 7.97–7.98 (m, 2H, H-3′ and H-5′), 7.96 (AA′BB′ system, 2H, $J_{10,11} = 5.6$ Hz, $J_{10,12} = 3.3$ Hz, H-10, H-13); 7.80 (AA′BB′ system, 2H, $J_{11,12} = 5.4$ Hz, $J_{11,13} = 3.2$ Hz, H-11, H-12); 6.94 (tt, 2H, $J = 9.04$ and 2.2 Hz, H-3′ and H-5′), 7.97–7.98 (m, 2H, H-2′ and H-6′), 5.16 (s, 2H, H-6 and H-6$_{6_t}$), 3.85 (s, 3H, CH_3O); ^{13}C NMR δ 173.33 (C-5), 168.28 (C-3), 166.92 (C-15), 161.96 (C-4′), 134.47 (C-10), 131.81 (C-9), 129.15 (C-2′, C-6′), 123.86 (C-11), 118.66 (C-1′), 114.13 (C-3′, C-5′), 55.32 (CH_3O), 33.58 (C-6). Anal. calcd for $C_{18}H_{13}N_3O_4$ (335.17): C, 64.48: H, 3.91; N, 12.53. Found: C, 64.97; H, 3.86; N, 12.47.

2.2.7. N-[3-(p-Chlorophenyl)-1,2,4-oxadiazol-5-yl-methyl]phthalimide (**6g**)

Crystallized from chloroform, yield 75%; mp 174 °C; IR (KBr): 1774, 1716, 1595, 1568, 1115 and 945 cm^{-1}; ^{1}H NMR ($CDCl_3$) δ 7.99–8.00 (m, 2H, H-2′ and H-6′), 7.98 (AA′BB′ system, 2H, $J_{10,11} = 5.2$ Hz, $J_{10,12} = 3.0$ Hz, H-10, H-13); 7.81 (AA′BB′ system, 2H, $J_{11,12} = 5.4$ Hz, $J_{11,13} = 3.0$ Hz, H-11, H-12); 7.42 (tt, 2H, $J = 8.70$ and 2.10 Hz, H-3′ and H-5′), 5.18 (s, 2H, H-6 and H-6$_{6_t}$); ^{13}C NMR ($CDCl_3$) δ 173.91 (C-5), 167.80 (C-3), 166.89 (C-15), 137.48 (C-4′), 134.55 (C-10), 131.76 (C-9), 129.09 (C-3′), 128.84 (C-2′, C-6′), 124.70 (C-1′), 123.91 (C-11), 33.54 (C-6). Anal. calcd for $C_{17}H_{10}N_3O_3Cl\cdot 1/2H_2O$ (344.20): C, 59.31; H, 3.07; N, 12.20. Found: C, 59.44; H, 2.91; N, 12.56.

2.3. Computational and other procedures

All quantum chemical calculations were performed with the standard AM1 [16] Hamiltonian implemented into the MOPAC 93 (revision 2) program [17]. All geometry optimizations were performed in Cartesian coordinates without any restriction or constraints, except in the reaction coordinate calculations. The convergence threshold for all geometry optimization calculations was 5×10^{-3} kJ mol^{-1} pm^{-1}. All extreme points in the potential energy surface with chemical relevance (reactants, products, intermediates and transition states) have been characterized by the calculation of the Hessian eigenvalues [18,19]. The ORTEP-III program [20] was used for visualization of the molecular structures. The partition coefficient octanol/water, in its logarithmic form, log P has been calculated with the CLOGP program [21], which uses the additive properties of a data base containing nearly 8,000 fragments to estimate the partition coefficient of a given organic molecule. All statistical analyses have been performed with the Ein*Sight program [22], including the correlation, regression and principal component analysis (PCA).

3. Results and discussion

3.1. Synthesis

Reaction of phthalic anhydride **1** with glycine **2** in a domestic microwave oven provided *N*-phthaloylglycine **3** in about 60% yield. The preparation of **3** by conventional heating has been reported earlier [23]. Its microwave-induced synthesis from **1** and **2** in a mixture of DMF and *N*-methylmorpholine has been described in the literature [24a]. Tetrachlorophthalimidoacetic acid has also been obtained from tetrachlorophthalic anhydride and glycine by microwave-assisted technique using diglyme as solvent [24b]. However, the literature does not describe the synthesis of phthaloylglycine from phthalic anhydride and glycine under solvent-free conditions. Our approach to synthesize **3** avoided the use of any solvent, thus reducing the work-up problem and is friendly to the environment. Reaction of **3** with arylamidoximes **4a–g** in the presence of dicyclohexylcarbodiimide (DCC) at room temperature affords intermediates **5a–g**, which on heating for an extended period of time furnishes **6a–g** (Fig. 2) [14].

The structures of compounds **6a–g** were determined with the help of infrared, NMR spectra and elemental analyses. Further, heating of **5a–g** lost water

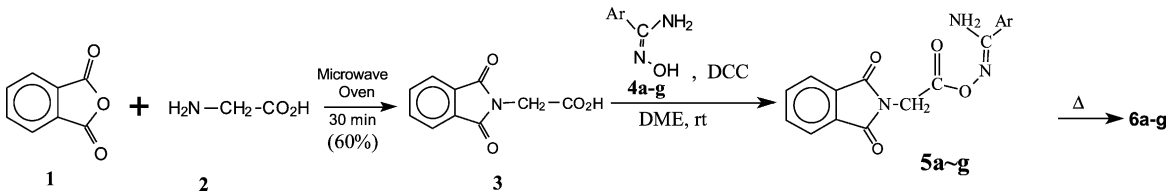

Fig. 2. Synthesis of new oxadiazolo-phthalimides.

and cyclized to provide 1,2,4-oxadiazoles without any other rearranged product. It is well known that heating of *O*-acylamidoximes furnish 1,2,4-oxadiazoles exclusively [25a,b]. Compounds **6a**–**g** possess interesting conformation. This is discussed in the section dealing with Molecular Conformation.

3.2. Pharmacology

Phthalimido-1,2,4-oxadiazoles are a new class of compounds and therefore **6a**–**g**, as first step, were tested for analgesic and antiinflammatory properties and found to possess such activities. The results are shown in Table 1 and have been published by us earlier [14].

3.3. Structure–activity relationships (SAR)

In order to better understand the biological activity of the newly synthesized oxadiazolo-phthalimides, we have attempted to establish some relationships between the activity, that is, ID_{50}, and molecular descriptors. A total of 14 substances have been tested and also calculated with quantum chemical method (AM1) and fragment (CLOGP) programs. These substances are shown in Table 2 and are grouped according to the substituents at positions 3 and 5 of the oxadiazole moiety.

As for the descriptors, we have chosen the following electronic and molecular properties calculated with the AM1 method: (i) lowest unoccupied molecular orbital energy, εLUMO; (ii) highest occupied molecular orbital energy, εHOMO; (iii) total dipole moment, μ; (iv) standard enthalpy of formation, ΔH_f; and (v) the net atomic charges, q. In order to take into account, at least partially, the effects of transport and migration through membranes, we have also calculated partition coefficients for the molecules, log P, as well as the hydrophobicity parameter of the substituents, $\pi(R_1)$ and $\pi(R_2)$. In addition, a topological descriptor, IR_1, indicating the presence (1) or absence (0) of the phthaloyl group has been considered, since this group is known to be important for the analgesic and antiinflammatory activities [13]. The descriptors and their calculated values are presented in Table 3. The atomic charges of 13 compounds are compiled in Table 4.

Table 1
Inhibition of acetic acid induced writhing in mice

Compound	Dose (mg/kg)	No. of tests	Inhibition of writhing (%)	ID_{50} (with 95% confidence limit)
Aspirin	200	3	38.2*	80.8 (50.8–103.0)
	100	3	61.7*	
	50	3	74.0	
6a	6.25	4	73.8*	
	3.12	3	67.1*	2.2 (1.4–3.5)
	1.56	3	38.9*	
6b	6.25	4	80.5*	
	3.12	3	76.5*	3.1 (2.1–4.6)
	1.56	3	$12.1^{N.S.}$	
6c	6.25	4	79.2*	
	3.12	3	67.1*	2.9 (1.9–4.4)
	1.56	3	25.5*	
6d	12.5	4	72.5*	7.2 (4.8–10.8)
	6.25	4	62.4*	
	3.12	3	$16.1^{N.S.}$	
6e	6.25	3	62.9*	4.1 (2.4–7.0)
	3.12	3	47.4*	
	1.56	3	$29.8^{N.S.}$	
6f	25.0	3	62.6*	14.9 (7.5–29.8)
	12.5	3	53.3*	
	6.25	3	41.9*	
	3.12	3	$20.7^{N.S.}$	
6g	25.0	3	59.6*	20.3 (11.3–36.5)
	12.5	3	$35.1^{N.S.}$	
	6.25	3	$16.3^{N.S.}$	

N.S. = not significant; * = significant.

Table 2
Molecular structures of the oxadiazole derivatives **6a–g**, **7–13**

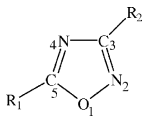

Substance	R_1	R_2
6a	Ar	Ph
6b	Ar	*o*-CH_3Ph
6c	Ar	*m*-CH_3Ph
6d	Ar	*p*-CH_3Ph
6e	Ar	*p*-NO_2Ph
6f	Ar	*p*-CH_3Oph
6g	Ar	*p*-ClPh
7	$-NH_2$	Ar′
8	$-NH-\underset{\underset{NH}{\|}}{C}-NH_2$	Ar′
9	Ar′	$-NH_2$
10	Ar′	–NHCHO
11	Ar′	–N=CHOEt
12	Ar′	$-H_2C-N(Me).HCl$
13	-$CH_2CH_2CO_2H$	Ph

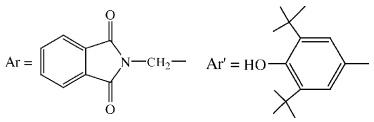

A correlation matrix between the experimental ID_{50} and all descriptors have been built (Table 5), which yielded the following largest correlation coefficients in decreasing order for each descriptor, log P : 0.506; ΔH_f : 0.394; μ : 0.268; q(C-5) : 0.239; and q(N-2) : 0.238. An initial multiple regression with these descriptors yielded a poor correlation with $r = 0.8$ and $F = 3.11$. As a result, we have performed a PCA of all compounds except **6g** on the data matrix containing all electronic and topological descriptors (Table 6). The PCA shows that only with three principal components (PC1, PC2 and PC3) it is possible to explain more than 82% of the original data. Also, PC1 alone explains nearly 53% of the original information, so that it would be appropriate to consider PC1 as a new descriptor, which contains all the electronic and topological information. As a result, the scores of PC1 with the physicochemical parameters log P and $(\log P)^2$ were used to construct a new statistical model for a multiple regression, which yielded the following values:

$$ID_{50} = -2.3(\pm 0.72)PC1 - 12.9(\pm 3.67)\log P + (\pm 0.59)(\log P)^2 + 40.2(\pm 5.37)$$

with $n = 13$; $r = 0.93$; $s = 3.18$ and $F_{3,9} = 18.1$.

This new model has a very high statistical significance. It also shows the importance of the partition coefficient, which has been taken into account according to the quadratic model of Hansch [26]. This model also presents a normal distribution of the residues, with the standard deviation of the residues within the $[\pm 2]$ range. Despite this model having a large statistical significance, and thus allowing for quantitative prediction, even though the number of molecules is limited, it does not yield direct information about the action mechanism of these compounds. This is due to the fact that all electronic topological information was compacted into the PC1. As a result, we have also performed some correlation analysis between ID_{50} and electronic descriptors and found that the net charge on the C-5 atom, q(C-5), seems to be relevant. For instance, a clustering of four groups has been identified as follows: (**12**; **6a**; **6b**; **6c**; **6d**; **6e**), (**7**; **8**; **9**; **10**; **11**), (**6f**; **6g**), (**13**). This clustering has also been observed for other descriptors, but not as evident as for q(C-5). These results suggest that the compounds with the best analgesic activity are those which have an electron-withdrawing group at the position 5 of the oxadiazole moiety and a weak electron-donating group at C-3. These correlations might be significant for a qualitative model for explaining the action mechanism of these compounds.

Regarding partition coefficients, it should be emphasized that the literature [27] reports that log P should be in the 0.7–2.0 range for an adequate transport through biological membranes. These trends were obtained from the studies with inhibitors of COX. However, if we check the calculated log P values for the present series (Table 2), we find that the most active compounds have log P values closest to the upper end of this optimal interval, that is, 2.0.

3.4. Interaction mechanism model

Although, we would like to carry out the experimental work involving phthalimides and COX-2 to confirm the inhibitory effect of this enzyme,

Table 3
Electronics, physicochemical and topological descriptors and ID_{50}

Compound	ID_{50}	εLUMO (eV)	εHOMO (eV)	μ (D)	ΔH_f (kcal/mol)	IR_1	log *P*	$\pi(R_1)$	$\pi(R_2)$
6a	2.2	−1.24	−9.45	3.13	64.72	1	2.70	0.50	2.15
6b	3.1	−1.25	−9.38	3.38	59.20	1	3.20	0.50	2.65
6c	2.9	−1.21	−9.35	4.51	56.07	1	3.20	0.50	2.65
6d	7.2	−1.23	−9.19	2.85	57.26	1	3.20	0.50	2.65
6e	4.1	−1.49	−10.21	8.99	69.16	1	2.45	0.50	1.2
6f	14.9	−1.22	−8.94	3.30	26.48	1	2.74	0.50	1.83
6g	20.3	−1.28	−9.41	4.44	57.75	1	3.42	0.50	2.75
7	4.70	−0.34	−9.12	3.40	7.40	0	4.72	−0.42	5.70
8	4.10	−0.54	−9.25	3.17	41.20	0	5.81	0	5.70
9	7.6	−0.73	−9.27	2.97	8.60	0	4.72	5.70	−0.42
10	6.3	−0.88	−9.20	5.47	−25.50	0	5.06	5.70	−0.45
11	8.2	−0.65	−9.02	3.99	−15.30	0	5.34	5.70	−0.52
12	6.9	−0.59	−9.00	3.57	9.60	0	4.61	5.70	−0.15
13	29.6	−0.61	−9.56	2.32	−26.20	0	0.90	−0.64	2.15

it is not possible at the moment because of the lack of the facility. It would also be interesting to carry out computational modeling studies to determine the proximity of the arginine residue with phthalimides. However, this is also difficult in our Department because no such program is available. Under the circumstance, we suggest the following theoretical work, which includes the electron-transfer mechanism and the transition state calculations of the enzyme–drug complex.

These models are based on the calculated molecular electronic parameters which permit to define the centers involved in the interaction of the phthalimide moiety of the molecule with the enzyme. AM1 calculations show that these phthalimide derivatives (**6a–g**) have high electron affinity (1.39–1.66 eV), indicating their capabilities to act as electrophiles. The low LUMO (lowest unoccupied molecular orbital) energy (−1.21 to −1.49 eV) confirms the eletrophilic character of carbonyl carbon. On the other hand, the active sites of both isoforms of COX contain arginine (Arg120) [28] besides other amino acid residues. Since arginine is an amino acid containing a guanidine group in its side-chain, guanidine has been selected as the appropriate electron donor. Indeed, the calculations show that it possesses a high HOMO (highest occupied molecular orbital) energy. The HOMO components are distributed in p_z of N1 (0.54), p_x of N in R2 (0.47) and p_y of N3 (0.35). Therefore, the present model consistently considers an electron transfer from the C=N of the enzyme to the carbonyl carbon as shown below (Scheme 1).

The above information leads to an intermediate state with charge separation which presumably forms an unstable four-membered ring. Consequently a N–C covalent bond, is formed as shown in intermediate A. Once a covalent bond is established between the nitrogen and carbonyl carbon atoms, the enzyme will suffer structural modification, thus

Table 4
Net atomic charges on the oxadiazole moiety calculated via AM1 method. See Table 2 for numbering

Substance	*q*(O-1)	*q*(N-2)	*q*(C-3)	*q*(N-4)	*q*(C-5)
6a	−0.073	−0.032	−0.039	−0.150	−0.012
6b	−0.075	−0.025	−0.043	−0.143	−0.019
6c	−0.080	−0.032	−0.036	−0.150	−0.016
6d	−0.075	−0.034	−0.038	−0.144	−0.017
6e	−0.065	−0.016	−0.058	−0.153	−0.003
6f	−0.073	−0.039	−0.034	−0.144	−0.019
6g	−0.070	−0.028	−0.044	−0.147	−0.019
7	−0.088	−0.098	−0.013	−0.187	−0.088
8	−0.100	−0.053	−0.010	−0.203	−0.133
9	−0.106	−0.059	−0.014	−0.212	−0.125
10	−0.086	−0.086	−0.044	−0.198	−0.109
11	−0.093	−0.011	−0.007	−0.211	−0.091
12	−0.088	−0.043	−0.032	−0.155	−0.020
13	−0.080	−0.031	−0.037	−0.160	−0.013

Table 5
Correlation matrix between ID_{50} and the descriptors

	ID_{50}	εLUMO	εHOMO	μ	ΔH_f	log P	IR_1	πR_1	πR_2	q(O-1)	q(N-2)	q(C-3)	q(N-4)	q(C-5)
ID_{50}	1.000													
εLUMO	0.108	1.000												
εHOMO	0.020	0.488	1.000											
μ	0.267	0.455	0.670	1.000										
ΔH_f	0.394	0.735	0.423	0.256	1.000									
log P	0.505	0.531	0.520	0.044	0.263	1.000								
IR_1	0.120	0.933	0.354	0.255	0.838	0.558	1.000							
πR_1	0.185	0.305	0.376	0.063	0.537	0.579	0.523	1.000						
πR_2	0.069	0.117	0.061	0.210	0.391	0.033	0.150	0.817	1.000					
q(O-1)	0.165	0.789	0.482	0.398	0.546	0.735	0.816	0.546	0.095	1.000				
q(N-2)	0.177	0.556	0.359	0.164	0.418	0.467	0.522	0.141	0.237	0.454	1.000			
q(C-3)	0.115	0.778	0.607	0.530	0.428	0.662	0.657	0.273	0.164	0.845	0.317	1.000		
q(N-4)	0.163	0.690	0.269	0.069	0.608	0.747	0.804	0.557	0.156	0.862	0.455	0.741	1.000	
q(C-5)	0.239	0.654	0.366	0.156	0.490	0.820	0.729	0.457	0.013	0.868	0.597	0.734	0.947	1.000

leading to the analgesic effect. Scheme 1 shows the possibility of the formation of final two products, C and D, where D represents the lower enthalpy of formation (47.03 kcal/mol). This kind of unsynchronized electron transfer mechanism is being suggested for the first time in this system. Such electron transfer reaction in others systems has been discussed by Pavão et al. [29].

To arrive to these products, two paths are proposed with their respective transition states $TS_n^{\ddagger}$ ($n = 1–5$), as shown in Scheme 2 for the cyclic and Scheme 3 for the acyclic ones.

The cyclic path, forming a six-atom transition state (TS1) is preferred because of hydrogen bonding ($d1 = 2.04$ Å; Scheme 2 and Table 5). The acyclic route (TS4) is unable to form the hydrogen bond ($d = 4.06$ Å; Scheme 3 and Table 5). The hydrogen bond in TS1 can also justify the lowest energy in that state (22.1 kcal/mol) as compared to the TS5 (30.6 kcal/mol), according to Fig. 3.

In addition, it can be noted that in the cyclic path (Scheme 2), even after the opening of the phtaloyl ring with N1 of arginine, the TS3 presents lower energy (28.6 kcal/mol) than the TS5 state (30.6 kcal/mol), as it can be seen in the Fig. 3. Once again, an intramolecular hydrogen bond seems to favor the TS3 state.

Considering that the carbonyl oxygen of the phthaloyl ring can form two intermolecular hydrogen bonds [30a–c], with other amino acid residues leading to enzyme modification. However, even so, TS1 would be favored because two hydrogen bonds would be formed: an intermolecular and other intramolecular. For the TS4 state it would just remain the possibility of intermolecular bonds, and the probability of formation of two hydrogen bonds with the active site is very small.

On the other hand, the TS3 and TS5 states present large atomic charge variations when compared with the reagents and TS1 (Table 7 and Schemes 2 and 3).

Table 6
Scores of the first three principal components analysis

Compound	PC1	PC2	PC3
6a	2.280	0.498	0.426
6b	2.342	0.526	0.491
6c	1.928	0.408	0.078
6d	1.879	0.905	1.068
6e	4.430	−1.871	−2.478
6f	1.447	0.551	1.379
7	−2.442	2.420	−1.206
8	−2.486	2.113	−1.430
9	−3.371	−1.136	−0.146
10	−2.025	−2.119	−0.788
11	−2.796	−1.608	0.820
12	−1.092	−1.114	1.432
13	−0.092	0.426	0.354

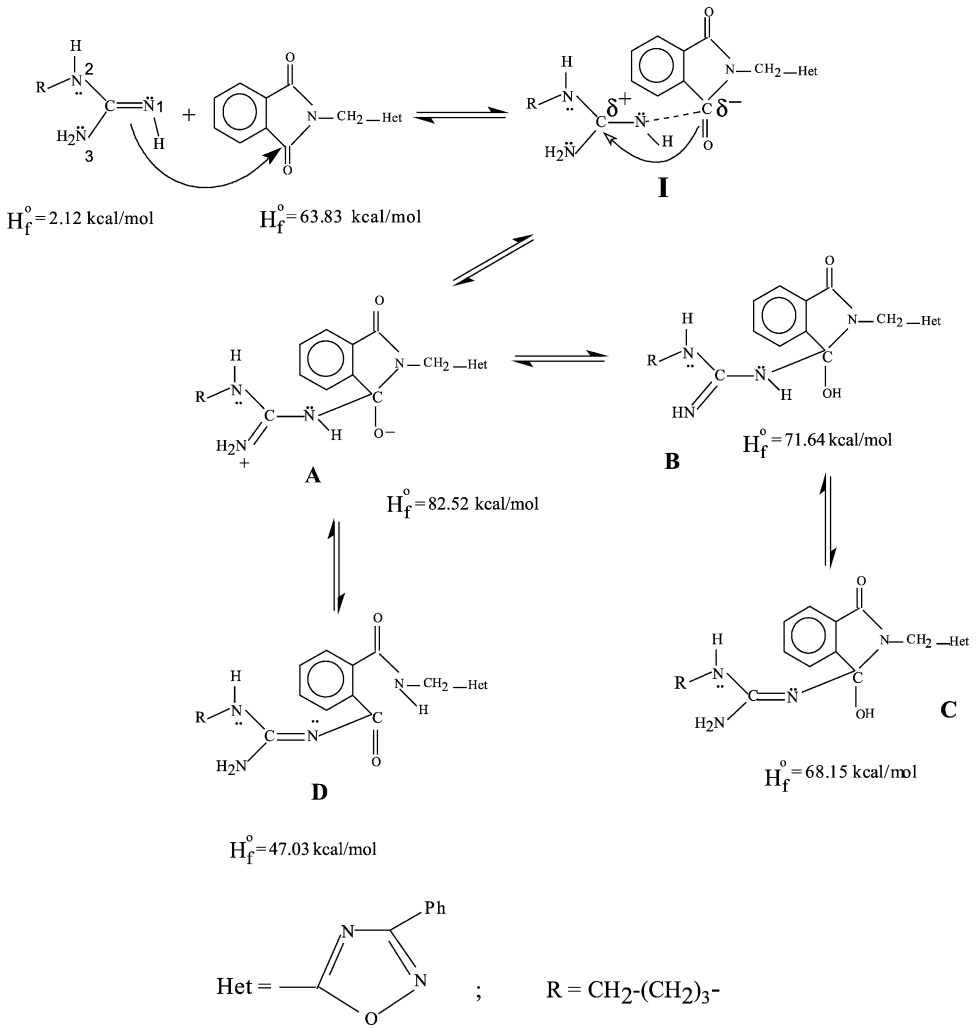

Scheme 1. Enthalpies of reagents and products.

The atomic charges can be stabilized by saline bridge and other electrostatic interactions with other amino acid residues of the active site, and once again TS3 will continue being the state more indicated to arrive to the product D. That is, besides being stabilized by the N15 and C2 interactions with the amino acid residues, a hydrogen intramolecular bond still exists ($d1 = 2.02$ Å).

In the cyclic path (Scheme 2), the TS2 presents higher energy (31.4 kcal/mol) than TS3 (28.6 kcal/mol), as shown in Fig. 4. It can therefore be noted that TS2 leads to the product C through a endothermic reaction (2.2 kcal/mol), while TS3 produces D for an exothermic reaction (− 18.9 kcal/mol). Therefore, the higher energy in TS2 could be due to the rigidity of the five-membered ring, with those atoms in the same plane, together with the instability of C5, which is a tetrahedral carbon bound to three heteroatoms. Thus, the Hammond's postulate can be applied here, which says that: 'in a reaction, with the same reagents and being arrived to two final products with different energy, the most stable product will also have a more stable transition state'. In that way, the path for the proposed nucleophilic reaction between arginine and

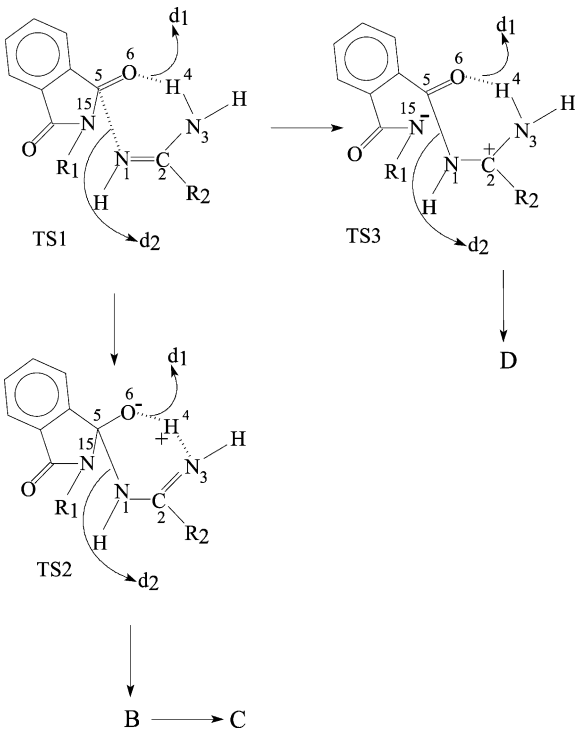

Scheme 2. Cyclic transition states.

carbonyl of the phthaloyl ring, taking into account the opening of the ring with the formation of the product D, goes by TS1 → TS3 → D.

3.5. Molecular conformation

The AM1 calculations also permit to predict the structures and conformations of phthalimide derivatives. The most stable conformations are those where the oxadiazol and phthalimide rings are almost perpendicular. The torsion angle C(8)–N(7)–C(6)–C(5) of **6a** is 84.35° (Fig. 5). On the other hand, the oxadiazol and the phenyl rings are almost coplanar, the N(2)–C(3)–C(16)–C17) torsion angle being 15.09° (Fig. 5). This is also observed for the *meta* and *para* substituents in the phenyl ring. However, the substituent in ortho position, as was expected, makes the phenyl ring out of the plane.

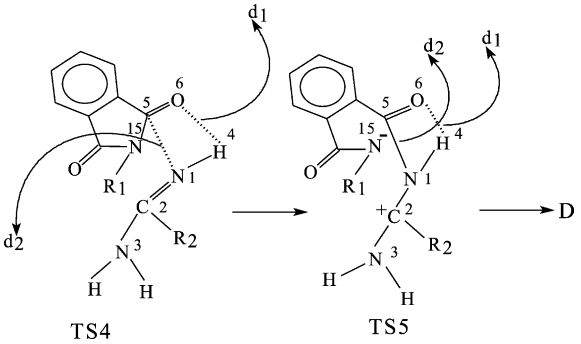

Scheme 3. Acyclic transition states.

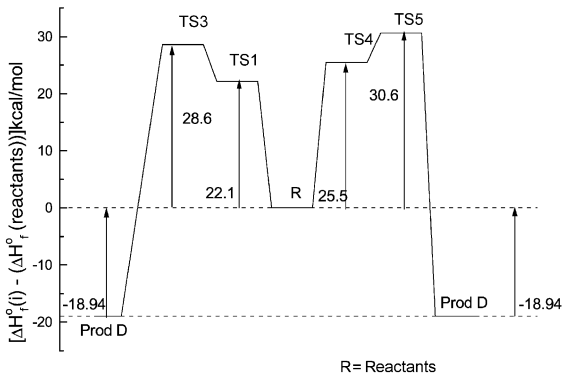

Fig. 3. Relative enthalpies of the transition states.

In order to verify the conformation of such compounds, we compared the X-ray work of the known compound, *N*-[3-(*p*-bromophenyl)-1,2,4-oxadiazol-5yl]methylphthalimide. This compound was prepared by us exactly in a similar manner as the others of this paper and the crystallographic data of

Table 7
Enthalpies, atomic charges (*q*) and distances (*d*) for the transition states

	TS1	TS2	TS3	TS4	TS5
H_f^0 (Kcal/mol)	88.04	97.36	94.57	91.41	96.51
*d*1 (Å)	2.04	1.36	2.02	4.06	3.98
*d*2 (Å)	1.72	1.51	1.49	1.72	1.49
q(N1)	−0.36	−0.32	−0.31	−0.35	−0.31
q(C2)	+0.30	+0.29	+0.36	+0.28	+0.38
q(N3)	−0.33	−0.38	−0.30	−0.35	−0.33
q(H4)	+0.27	+0.37	+0.30	+0.25	+0.27
q(C5)	+0.46	+0.38	+0.46	+0.45	+0.43
q(O6)	−0.51	−0.53	−0.44	−0.46	−0.41
q(N15)	−0.38	−0.38	−0.52	−0.37	−0.52
Relative H_f^0(Kcal/mol)	22.1	31.4	28.6	25.5	30.6

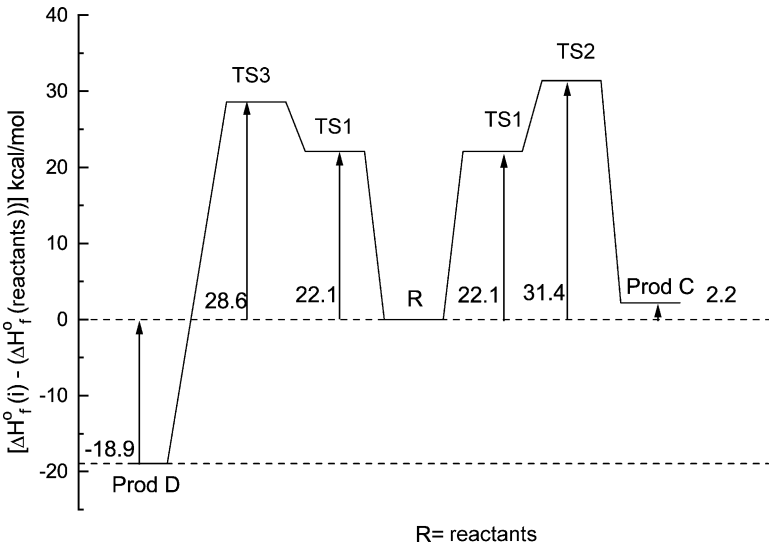

Fig. 4. Relative enthalpies leading to C and D products in the cyclic path.

a single crystal were collected and published [32]. The ORTEP diagram of this compound is shown in Fig. 6. Here, the torsion angle C(5)–C(6)–N(7)–C(8) is 104.93° showing that the oxadiazole ring is somewhat perpendicular to the phthalimide ring. The X-ray result also shows that the phenyl and oxadiazole rings are coplanar. Semi-empirical and ab initio calculations of this compound showed similarity with X-ray results [31]. In summary, the calculated and experimental results show similar conformations for compound *N*-[3-(*p*-bromophenyl)1,2,4-oxadiazol-5-yl]methylpthalimide.

Classic inhibitors of COX-1 (ibuprophen, indomethacin, naproxen, sulindac, etc.) and even the specific inhibitors for COX-2 [SC-581, SC-558, SC-58635 (CELECOXIB), Meloxicam, Dup 697, etc.] more recently studied [32–34], act through mechanisms which could be based on electrons transfer or

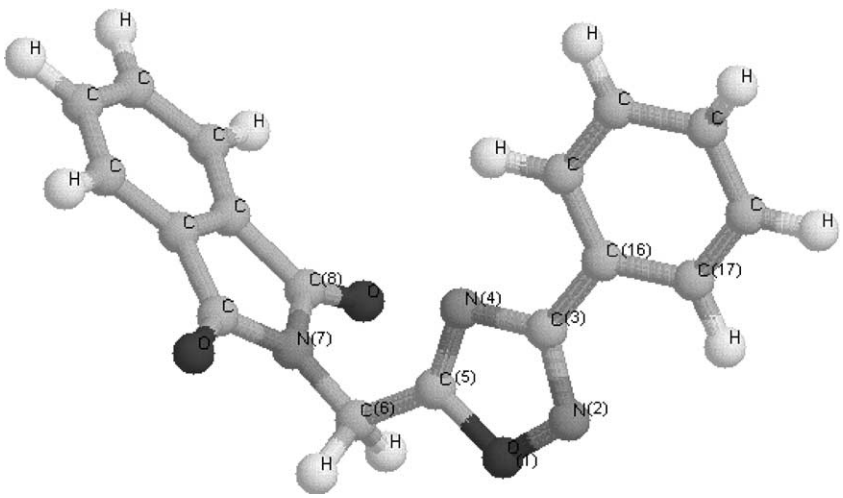

Fig. 5. The most stable conformation for the oxadiazolo-phthalimide.

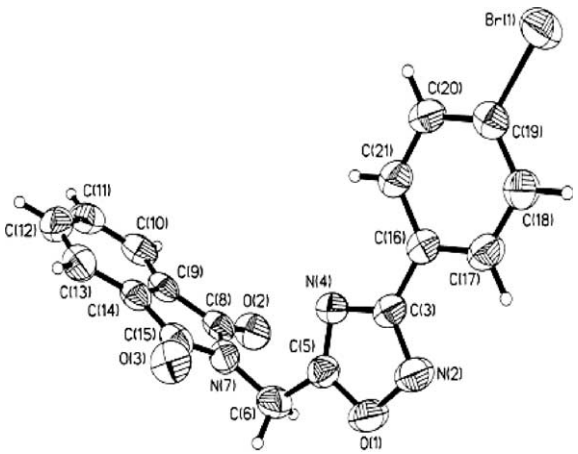

Fig. 6. ORTEP diagram.

through hydrogen bond interactions. It is important to highlight that until the present moment, aspirin is the only analgesic capable of covalently binding to the enzyme, and therefore, capable to inhibit it in an irreversible way. All other analgesics, including the classical and the specific inhibitors for COX-2, act in a reversible way, through the interactions mentioned above.

In conclusion, we would like to say that we have explained the characterization of seven compounds **6a–g** [14]. We are also suggesting the interaction mechanism between these compounds and the enzyme COX-2. Also, the Resonance Valence Bond theory led us to propose, for the first time, an entirely new mechanism involving an electron transfer from the amino acid residue of the enzyme to the drug. It was also possible to calculate the transition states involving the drug and the enzyme and we found that TS1 has lower energy than other transition states. Besides, we also calculated the approximate volume of the synthesized compounds and found them to be 385 $Å^3$, which makes it possible to fit in the active site cavity of COX-2 cavity which has a volume [29] of 394 $Å^3$.

Acknowledgements

We are grateful to the Brazilian National research Council (CNPq), and to Program for Improvement of the Personnel at Higher Level (CAPES) for financial assistance.

References

[1] A. Korolkovas, J.H. Burckhater, Química Farmacêutica, Guanabara Koogan, Rio de Janeiro, 1988, pp. 159–217.
[2] S.H. Ferreira, Nat. New Biol. 240 (1972) 200.
[3] J.R. Vane, Nat. New Biol. 231 (1971) 232.
[4] F.J. Van gives Ouderaa, M. Buytenhek, D.H. Nugteren, D.A. Van Dorp, Eur. J. Biochem. 109 (1980) 1.
[5] J.R. Vane, R.J. Flower, R.M. Botting, Stroke 21 (1990) 12.
[6] T.A. Samad, K.A. Moore, A. Sapirstein, S. Billet, A. Allchorne, S. Poole, J.V. Bonventre, C.J. Woolf, Nature 410 (2001) 471.
[7] G.M. Pasinetti, Arch. Gerontol. Geriatr. (2001) 3.
[8] W. Dempke, C. Rie, A. Grothey, H.J. Schmoll, J.Cancer Res. Clin. Oncol. 127, p. 411, 2001.
[9] A.S. Kalgutkar, Z. Zhao, Curr. Drug Target. 2 (2001) 79.
[10] P. Afiatpour, R.M. Srivastava, M.L. de Oliveira, E.J. Barreiro, Braz. J. Med. Biol. 27 (1994) 1403.
[11] J. Sheskin, J. Clin. Pharmacol. Ther. 6 (1965) 303.
[12] C.L. Crawford, Adv. Drug React. Toxicol. Rev. 13 (1994) 177.
[13] G.W. Muller, L.G. Corral, M.G. Shire, H. Wang, A. Moreira, G. Kaplan, D.I. Stirling, J. Med. Chem. 39 (1996) 3238.
[14] R. Antunes, H. Batista, R.M. Srivastava, G. Thomas, C.C. Araújo, Bioorg. Med. Chem. Lett. 8 (1998) 3071.
[15] R. Antunes, R.M. Srivastava, Heterocycl. Commun. 2 (1996) 247.
[16] M.J.S. Dewar, E.G. Zoebisch, E.F. Healy, J.J.P. Stewart, J. Am. Chem. Soc. 107 (1985) 3902.
[17] J.J.P. Stewart, MOPAC 93.00 Manual, Fujitsu Limited, Tokyo, Japan, 1993.
[18] W.J. Hehre, L. Radom, P.R. Schleyer, J.A. Pople, Ab initio Molecular Orbital Theory, Wiley, New York, 1986.
[19] T. Clark, A Handbook of Computational Chemistry, Wiley, New York, 1985.
[20] M.N. Burnett, C.K. Johnson, ORTEP-III, Oak Ridge National Laboratory, Oak Ridge, TN, USA, 1996.
[21] A. Leo, Chem. Rev. 93 (1993) 1281.
[22] Ein*Sight 3.0 Infometrix, 2200 Sixth Avenue, Suite 833, Seattle, WA 98121.
[23] J.H. Bilman, W.F. Harting, J. Am. Chem. Soc. 70 (1948) 1473.
[24] (a) S.S. Bari, A.K. Bose, A.G. Chaudhary, M.S. Manhas, V.S. Raju, E.W. Robb, J. Chem. Educ. 69 (1992) 938. (b) A.K. Bose, M. Jayaraman, A. Okawa, S.S. Bari, E.W. Robb, M.S. Manhas, Tetrahedron Lett. 37 (1996) 6989.
[25] (a) R.M. Srivastava, F.J.S. Oliveira, D.S. Machado, R.M. Souto-Maior, Synth. Commun. 29 (1999) 1437. (b) L.B. Clapp, A.R. Katritzky,Advanced in Heterocyclic Chemistry vol. 20Academic PressNew York (1976) 65–116.
[26] C. Hansch, T. Fujita, J. Am.Chem. Soc. 86 (1964) 1616.
[27] P. Moser, A. Sallmann, I. Wiesenberg, J. Med. Chem. 33 (1990) 2358.

[28] R.G. Kurumbail, M.A. Stevens, J. Gierse, J.J. McDonald, R.A. Stegeman, J.Y. Pak, D. Gildehans, J.M. Miyshiro, T.O. Penning, K. Seibert, P.C. Isackson, W.C. Stallings, Nature 384 (1996) 644.
[29] A.C. Pavão, C.A. Taft, T.C.F. Guimarães, M.B.C. Leão, J.R. Mohallem, W.A. Lester Jr., J. Phys. Chem. A 105 (2001) 5 and the references cited therein.
[30] (a) J.D. Mature, W.L. Jorgensen, J. Am. Chem. Soc. 108 (1986) 2517. (b) J.F. Blake, W.L. Jorgensen, J. Am. Chem. Soc. 109 (1987) 3856. (c) W.L. Jorgensen, J. Am. Chem. Soc. 111 (1989) 3770.
[31] H. Batista, G.B. Carpenter, R.M. Srivastava, J. Chem. Cristallog. 30 (2000) 131.
[32] D. Picot, P.J. Loll, R.M. Garavito, Nature 367 (1994) 243.
[33] P.J. Loll, D. Picot, R.M. Garavito, Nat. Struct. Biol. 2 (1995) 637.
[34] L.S. Simon, F.L. Lanza, P.E. Lipsky, R.C. Hubbard, S. Talwalker, B.D. Schwartz, P.C. Isackson, G.S. Geis, Arthritis Rheum. 41 (1998) 1591.